Vascular remodelling and fibrotic changes in the joint capsule during periprosthetic knee infections

From Charité–Universitätsmedizin Berlin, Corporate Member of Freie Universität Berlin, Humboldt-Universität zu Berlin, and Berlin Institute of Health, Berlin, Germany

Cite this article:
Bone Joint Res 2026;15(2):
121–134.

DOI: 10.1302/2046-3758.
152.BJR-2025-0203.R1

Correspondence should be sent to Arne Kienzle arne.kienzle@charite.de

R. Qiao,[1,2] J. Mehl,[2] B. Qi,[3] E. Sistemich,[1,2] W. Fan,[1] S. Kirschbaum,[1] S. Donner,[1] M. Thiele,[2] D. Jahn,[2,4] C. Gwinner,[1] G. Duda,[2] C. F. Perka,[1] A. Kienzle[1,2,5]

[1]Center for Musculoskeletal Surgery, Clinic for Orthopedics, Charité–Universitätsmedizin Berlin, Corporate Member of Freie Universität Berlin, Humboldt-Universität zu Berlin, and Berlin Institute of Health, Berlin, Germany
[2]Julius Wolff Institute and Center for Musculoskeletal Surgery, Charité–Universitätsmedizin Berlin, Corporate Member of Freie Universität Berlin, Humboldt-Universität zu Berlin, and Berlin Institute of Health, Berlin, Germany
[3]Institute of Stomatology, Chinese People's Liberation Army No.989 Hospital, Luoyang, China
[4]Department of Oral and Maxillofacial Surgery, Charité–Universitätsmedizin Berlin, Corporate Member of Freie Universität Berlin, Humboldt-Universität zu Berlin, and Berlin Institute of Health, Berlin, Germany
[5]Berlin Institute of Health at Charité–Universitätsmedizin Berlin, BIH Biomedical Innovation Academy, Berlin, Germany

Aims

Periprosthetic joint infection (PJI) represents one of the most severe complications following joint arthroplasty, often associated with a high recurrence rate despite appropriate therapeutic interventions. The underlying mechanisms contributing to this persistent risk remain incompletely understood. We hypothesize that alterations in joint capsule vascularization and fibrotic remodelling contribute to the pathophysiology of PJI and its recurrence.

Methods

A total of 69 patients undergoing joint arthroplasty surgery were included in the study (21 controls: primary total knee arthroplasty (TKA), 22 PJI revision: explantation, and 26 PJI revision: prosthesis reimplantation after temporary arthrodesis). Each knee joint capsule specimen was analyzed using haematoxylin and eosin (HE) staining, Masson's trichrome, Sirius red staining, immunofluorescence staining, and real-time quantitative polymerase chain reaction (RT-qPCR).

Results

Mean vessel area, diameter, and perimeter were reduced in PJI specimens, despite an overall increase in the number of blood vessels. A significant reduction in smooth muscle cell (SMC) and pericyte layer thickness, along with decreased pericyte coverage of vessel walls, was observed following both explantation and reimplantation. Fibrotic remodelling, indicated by increased collagen deposition, was markedly elevated in PJI samples at both stages. Gene expression analysis revealed upregulation of PDGFB, MIG, MMP-9, and COL1A1 at explantation or reimplantation, while PDGFA and FN1 were downregulated at explantation and significantly upregulated at reimplantation. VEGFA and FGF-2 expression remained consistently suppressed.

Conclusion

PJI is associated with profound vascular remodelling and fibrotic transformation of the joint capsule, marked by aberrant angiogenesis, disrupted vessel architecture, and distinct gene expression profiles. These alterations may impair tissue perfusion, compromise immune surveillance, and hinder antibiotic delivery, thereby contributing to recurrent infection. Targeting soft-tissue vascularization and fibrosis may represent a novel therapeutic strategy to reduce PJI recurrence and enhance surgical outcomes.

Bone & Joint Research

Introduction

Periprosthetic joint infection (PJI) remains one of the most serious complications following joint arthroplasty, imposing a substantial burden on patients and healthcare systems worldwide.[1–3] Despite advancements in prosthesis design, aseptic surgical techniques, and antibiotic regimens, the incidence of PJI following knee arthroplasty remains at approximately 1% to 5%.[3–8] Even after successful treatment, long-term complications are frequent, with aseptic loosening and recurrent PJI occurring in up to 16% and 22% of cases, respectively.[9] Previous research revealed that roughly half of relapsing infections are caused by the same pathogen, while the other half involve new microbial species.[9] Although pathogen persistence has been implicated in same-pathogen PJI recurrence,[10,11] the precise mechanisms underlying reinfection remain incompletely understood. Several risk factors, including sex and comorbid cardiac or psychiatric conditions, have also been associated with increased recurrence rates.[12] The knee joint capsule, a fibrous envelope that contributes to joint stability and serves as a conduit for synovial vasculature, becomes particularly important after total knee arthroplasty (TKA), where it constitutes the primary soft-tissue interface with vascular access once the joint surfaces are covered by metal implants. In this capacity, the capsule is central to wound healing, immune surveillance, and antibiotic delivery.[13–16] Nevertheless, the pathological mechanisms contributing to the high failure rates observed after revision surgery for PJI are still largely unexplored.

Recent studies, including our own, have demonstrated a pronounced inflammatory response within the bone and synovial fluid of PJI patients, characterized by elevated inflammatory cytokine levels and an increased proportion of polymorphonuclear cells.[17–19] While an initial inflammatory response is essential for tissue regeneration and remodelling, persistent chronic inflammation has been demonstrated to negatively impact neovascularization as well as bone and soft-tissue regeneration.[20–23] Clinical series have also reported poor outcomes in specific patient groups such as octogenarians, fungal PJI, and staged revision procedures, pointing to the multifactorial nature of infection-associated inflammation-dependent tissue remodelling.[24–28] We hypothesize that these inflammatory changes also extend to the knee joint capsule, leading to fibrosis and alterations in vascularization. Such changes may compromise immune surveillance and antibiotic delivery to the joint by disrupting the structural integrity and function of the vascular network. Ultimately, this impaired vascular environment could weaken the immune response, increasing the risk of recurrent PJI.

In this study, we investigated whether PJI leads to persistent alterations in the vascular and fibrotic architecture of the knee joint capsule that may contribute to reinfection risk. These findings may provide insights into the pathological remodelling of the periprosthetic soft-tissue environment and identify potential targets for improving long-term outcomes in PJI.

Methods

Patients

This study was approved by the institutional ethics committee of Charité University Hospital (EA2/083/19) and conducted in accordance with the Declaration of Helsinki.[29] Written informed consent was obtained from all participants prior to surgery. Patients undergoing two-stage revision TKA for PJI at Charité were included. A control group of patients receiving primary TKA for osteoarthritis was included for comparison.

Eligibility for TKA reimplantation was based on the European Bone and Joint Infection Society (EBJIS) criteria: in addition to the absence of symptoms of infection for a minimum of six weeks following implant removal, individuals were required to demonstrate negative CRP and white blood cell counts.[30] The exclusion criteria included non-primary osteoarthritis, HIV infection, and initial TKA caused by trauma or infection.

In total, 69 knee joint capsule samples were analyzed: 21 from control patients (Con), 22 from patients at the time of prosthesis explantation (Ex), and 26 from reimplantation (Re). Clinical variables included age, sex, BMI, American Society of Anesthesiologists (ASA) grade,[31] infecting organism, and the Krenn-Morawietz histopathological classification system for septic versus aseptic prosthesis failure.[32]

Patient characteristics

This study analyzed joint capsule tissue from 69 patients undergoing knee surgery, including 40 males (58%) and 29 females (42%), with a mean age of 68.9 years (standard error of the mean (SEM) 9.4) and a mean BMI of 29.3 kg/m^2 (SEM 4.8). The median ASA grade was II, and all patients presented with at least two comorbidities. No significant differences were observed in baseline or perioperative characteristics across the groups (Table I). At the time of prosthesis implantation, most tissue samples were classified as Krenn-Morawietz classification grade 2 (44.9% (n = 31)) or grade 3 (27.5% (n = 19)). The predominant pathogens identified were *Staphylococcus aureus*, *Staphylococcus epidermidis*, and *Staphylococcus hominis* (Supplementary Table i). While sex distribution differed between groups, no clear sex-specific differences in vascular or fibrotic parameters were observed within the available cohort.

Sample preparation

During primary TKA, explantation, or reimplantation procedures, a soft-tissue specimen measuring approximately 5 × 5 × 1 to 2 mm was harvested from the anterior knee joint capsule, adjacent to the suprapatellar pouch. Tissue was excised from redundant anterior capsule during arthrotomy. Samples were rinsed with Ringer's solution (B. Braun SE, Germany) to remove blood and subsequently divided into three parts: one was stored in RNAlater (Ambion, USA) for gene expression analysis, one was fixed in 4% paraformaldehyde (PFA) and paraffin-embedded for histological staining, and one was embedded in super cryo-embedding medium (SCEM) and snap-frozen for immunofluorescence.

Histological staining

Samples were fixed in 4% PFA for 48 hours and dehydrated through a graded ethanol series (70% for 1 hr, 80% for 1 to 2 hrs, 96% for 2 × 2 hrs, and 100% for 2 × 2 to 3 hrs). Tissue was then cleared in xylene (twice for 1 hr and 1.5 hrs) and infiltrated with paraffin (twice for 2 hrs) using an automated tissue processor (Leica TP1020; Leica

Biosystems, Germany). Tissue sections of 4 μm each were cut using a Leica RM2235 manual rotary microtome. For all stains, sections were deparaffinized in xylene (2 × 10 mins), rehydrated through descending ethanol (100%, 96%, 80%, 70%; 2 mins each), and rinsed in distilled water. Haematoxylin & Eosin (H&E) staining was performed by incubating sections in Harris's haematoxylin (Merck, Germany) for seven minutes, followed by differentiation in 0.25% HCl–ethanol, washing in tap water for ten minutes, counterstaining with 0.2% eosin (Chroma Waldeck, Germany) for two minutes, dehydration, clearing, and mounting. For Sirius Red staining, rehydrated sections were incubated in 1% Sirius Red (Biebrich scarlet–acid fuchsin in saturated picric acid; Sigma-Aldrich, USA) for one hour, rinsed in 0.5% acetic acid, washed in running water, dehydrated, cleared, and mounted. The Trichrome (Modified Masson's; ScyTek, USA) staining was carried out by sequential incubation in Weigert's haematoxylin, Biebrich scarlet-acid fuchsin, phosphotungstic/phosphomolybdic acid, and aniline blue, followed by dehydration, clearing, and coverslipping.

Imaging was performed with a Leica DM6B microscope (Leica Microsystems, Germany) at 10× magnification to generate mosaic images. Quantitative histological analysis was performed on H&E-, Sirius Red-, and Masson's trichrome-stained sections. From each mosaic image, ten non-overlapping regions of interest (ROIs) with an approximate size of 0.5 × 0.5 mm were randomly selected. Cell counts were performed within each ROI. Collagen area (Sirius Red and Masson) was quantified using ImageJ (National Institutes of Health, USA) with colour thresholding and expressed as percentage of stained area relative to total tissue area. All analyses were performed independently by two blinded observers (RQ, BQ).

Immunofluorescence staining

PFA-fixed tissue was embedded in super cryo-embedding medium (SCEM) and snap-frozen in chilled hexane (Carl Roth, Germany). Sections (7 μm) were prepared using a Leica CM3050S cryostat and mounted with Cryofilm type II C (Section Laboratory, Japan). Blocking was performed for 60 minutes in phosphate-buffered saline (PBS) containing 3% bovine serum albumin (BSA) and 5% normal serum (host species of the secondary antibody: goat or donkey). The blocking reagent was chosen according to the primary antibody. Sections were incubated overnight at 4°C with primary antibodies diluted in Dako Antibody Diluent (Agilent, #S0809): CD31/PECAM1 (1:200, 910005, BioLegend), Endomucin (1:200, bs-4808R, Thermo Fisher, USA), α-SMA (1:400, M0851, Dako), CD146 (1:200, ab75769, Abcam), Fibronectin (1:200, MA5-11981, Thermo Fisher), and Collagen I (1:400, ab138492, Abcam). The next day, sections were washed (3 × 5 mins in PBS), then incubated with secondary antibodies for one hour at room temperature (goat anti-mouse Alexa Fluor 555 (1:400, A32727, Thermo Fisher), donkey anti-rabbit Alexa Fluor 647 (1:400, 406414, BioLegend)). Slides were mounted in Fluoromount-G with 4′,6-diamidino-2-phenylindole (DAPI) (SouthernBiotech, USA). Images were acquired with a Leica DM6B microscope at 20× magnification. All images were acquired under identical microscope settings (exposure time, gain, and laser intensity) to ensure comparability of fluorescence signals between groups. Quantitative analysis was performed using a custom ImageJ plugin. For each section, ten randomly selected ROIs with a size of 1 × 1 mm were analyzed. Vessel morphology (number, area, diameter, perimeter) was quantified after manual outlining of vessel boundaries. Pericyte and smooth muscle cell coverage/thickness were calculated relative to endothelial boundaries. Fibronectin and collagen I were measured as mean fluorescence intensity. All analyses were performed by two independent blinded observers (RQ, BQ).

Gene expression analysis

Tissue samples were homogenized in TRIzol (Sigma Aldrich, USA) with an Ultra Turrax homogenizer (IKA). RNA was extracted by chloroform separation, isopropanol precipitation, and ethanol washes, followed by purification on NucleoSpin RNA columns (Macherey-Nagel, Germany). RNA yield and purity were assessed with a NanoDrop spectrophotometer (USA). For reverse transcription, 1 μg RNA was converted into cDNA using the High-Capacity cDNA Reverse Transcription Kit (Thermo Fisher) under the following conditions: 65°C for five minutes, 42°C for 60 minutes, and 70°C for five minutes. qPCR was performed on a QuantStudio 5 Real-Time PCR System with Power SYBR Green Master Mix (Thermo Fisher). Cycling conditions were as follows: 95°C for ten minutes, 40 cycles of 95°C for 15 seconds, and 60°C for 60 seconds, followed by melt curve analysis.

Primers were designed from NCBI RefSeq sequences, with accession numbers listed in Table II. Glyceraldehyde 3-phosphate dehydrogenase (GAPDH) was used as the reference gene, in line with previous studies on musculoskeletal tissues where its expression was shown to be stable.[18,19] In the present dataset, GAPDH Ct values did not display substantial variability across groups, supporting its suitability as a normalizer. Primer efficiencies (90% to 110%) were validated using standard curves. Fold changes were calculated using the 2^−ΔΔCt (Livak) method. All qPCR experiments followed MIQE guidelines.[33]

Statistical analysis

Data were recorded in Microsoft Excel 2019 (Microsoft, USA) and analyzed using GraphPad Prism (v8.0.2; GraphPad Software, USA). Normality was tested with the Shapiro-Wilk test. Depending on data distribution, comparisons were made using one-way analysis of variance (ANOVA) for normally distributed variables or the Kruskal-Wallis test for non-normal data. Results are reported as means or medians with SEM. A p-value < 0.05 was considered statistically significant.

Results

Increased cellular presence in soft-tissue specimens

Haematoxylin and eosin (H&E) staining of soft-tissue specimens collected during surgery revealed a marked increase in cell count (Figure 1): at the time of prosthesis removal, there was a statistical trend to elevated cell counts at 316.2 cells per mm^2 (SEM 49.81 (95% CI 212.0 to 420.5)) compared to the control group at 166.4 cells per mm^2 (SEM 30.22 (95% CI 102.9 to 229.9); p = 0.140, Kruskal-Wallis test). Upon reimplantation, the cell count was further increased to 426.4 cells per mm^2 (SEM 50.12 (95% CI 322.9 to 529.8); p < 0.001, Kruskal-Wallis test), which was significantly higher than controls.

Table I. Patient characteristics.

Characteristic	Control	PJI (explantation)	p-value*	PJI (reimplantation)	p-value*
All patients, n	21	22		26	
Mean age, yrs (range)	70.1 (55 to 80)	68.8 (49 to 91)	0.949	67.9 (49 to 85)	0.706
Sex, n					
Male	8	15	0.087	17	0.116
Female	13	7		9	
Clinical scores					
Mean BMI, kg/m^2 (range)	28.3 (22 to 37)	30.1 (25 to 44)	0.424	29.4 (20 to 44)	0.701
ASA grade, n					0.751
I	3	0	0.609	0	
II	13	15		15	
III	5	7		10	
IV	0	0		1	

*One-way analysis of variance.

Table II. Real-time quantitative polymerase chain reaction primer.

Gene	Accession No.	Sense primer	Anti-sense primer
VEGFA	NM_001025366.3	5′-CCATGGCAGAAGGAGGAG-3′	5′-CACAGGATGGCTTGAAGA-3′
PDGFA	NM_001395363.1	5′-AGTCAGATCCACAGCATCCG-3′	5′-GCTCTCAGGCTGGTGTCC-3′
PDGFB	NM_002608.4	5′-ATGATCTCCAACGCCTGCT-3′	5′-TCCTTCTTCCACGAGCCAAG-3′
MIG	NM_002416.3	5′-AAGCCCTTCCTGCGAGAAA-3′	5′-TCACATCTGCTGAATCTGGGT-3′
MMP-9	NM_004994.3	5′-TCTTCCCTGGAGACCTGAGA-3′	5′-ATTTCGACTCTCCACGCATC-3′
COL1A1	NM_000088.4	5′-GGATCCATATGCAGACCTCAGAA-3′	5′-CTCCTTCCATGATCATTCCGGT-3′
FN-1	NM_001306129.2	5′-GCATTGCCAACCTTTACAGACC-3′	5′-AGTTGGGCTGACTCGGAGT-3′
FGF-2	NM_001361665.2	5′-CCACTTCAAGGACCCCAAGC-3′	5′-ACACAACTCCTCTCTCTTCTG-3′
GAPDH	NM_001256799.3	5′-CTGCACCACCAACTGCTTAG-3′	5′-ACAGTCTTCTGGGTGGCAGT-3′

COL1A1, type I collagen; FGF-2, fibroblast growth factor 2; FN-1, fibronectin 1; GAPDH, glyceraldehyde 3-phosphate dehydrogenase; MMP, matrix metalloproteinase; PDGFA, platelet-derived growth factor subunit A; PDGFB, platelet-derived growth factor subunit B; VEGFA, vascular endothelial growth factor A.

Alterations in blood vessel density and morphology

Double staining for platelet endothelial cell adhesion molecule-1 (PECAM-1/CD31) and endomucin (EMCN) revealed a significant increase in blood vessel density (Figure 2). At the time of prosthesis reimplantation, the number of blood vessels was elevated to 12.87 vessels per mm^2 (SEM 3.19 (95% CI 6.24 to 19.50)), compared to both the control group at 2.50 vessels per mm^2 (SEM 0.83 (95% CI 0.75 to 4.26); p = 0.045) and the explantation group at 4.47 vessels per mm^2 (SEM 0.79 (95% CI 2.80 to 6.14); p < 0.001). Despite this increase in vessel quantity, the mean vessel area was significantly reduced during both prosthesis explantation and reimplantation, measuring 1,032 μm^2 (SEM 174.9 (95% CI 661.3 to 1,403); p = 0.002) and 675.9 μm^2 (SEM 99.59 (95% CI 468.8 to 883); p = 0.003), respectively, compared to the control group at 4,838 μm^2 (SD 1,295 (95% CI 2,093 to 7,582)). Similarly, vessel diameter showed a substantial decline, decreasing to 34.41 μm (SEM 2.85 (95% CI 28.38 to 40.45); p = 0.002) during explantation and further to 28.03 μm (SEM 1.89 (95% CI 24.11 to 31.96); p < 0.001) at reimplantation, in contrast to the control group's 70.34 μm (SEM 8.71 (95% CI 51.88 to 88.79)). Additionally, the vessel perimeter was significantly reduced throughout both phases, measuring 118.3 μm (SEM 10.8 (95% CI 95.4 to 141.2); p = 0.002, all Kruskal-Wallis test) during prosthesis explantation and further decreasing to 99.91 μm (SEM 7.40 (95% CI 84.51 to 115.3); p < 0.001) at reimplantation, compared to the control group's 223.1 μm (SEM 25.93 (95% CI 168.2 to 278.1)).

Reduction in pericyte and smooth muscle cell coverage

Co-staining for CD31 and CD146 (Figure 3) revealed significant changes in pericyte thickness at the time of prosthesis

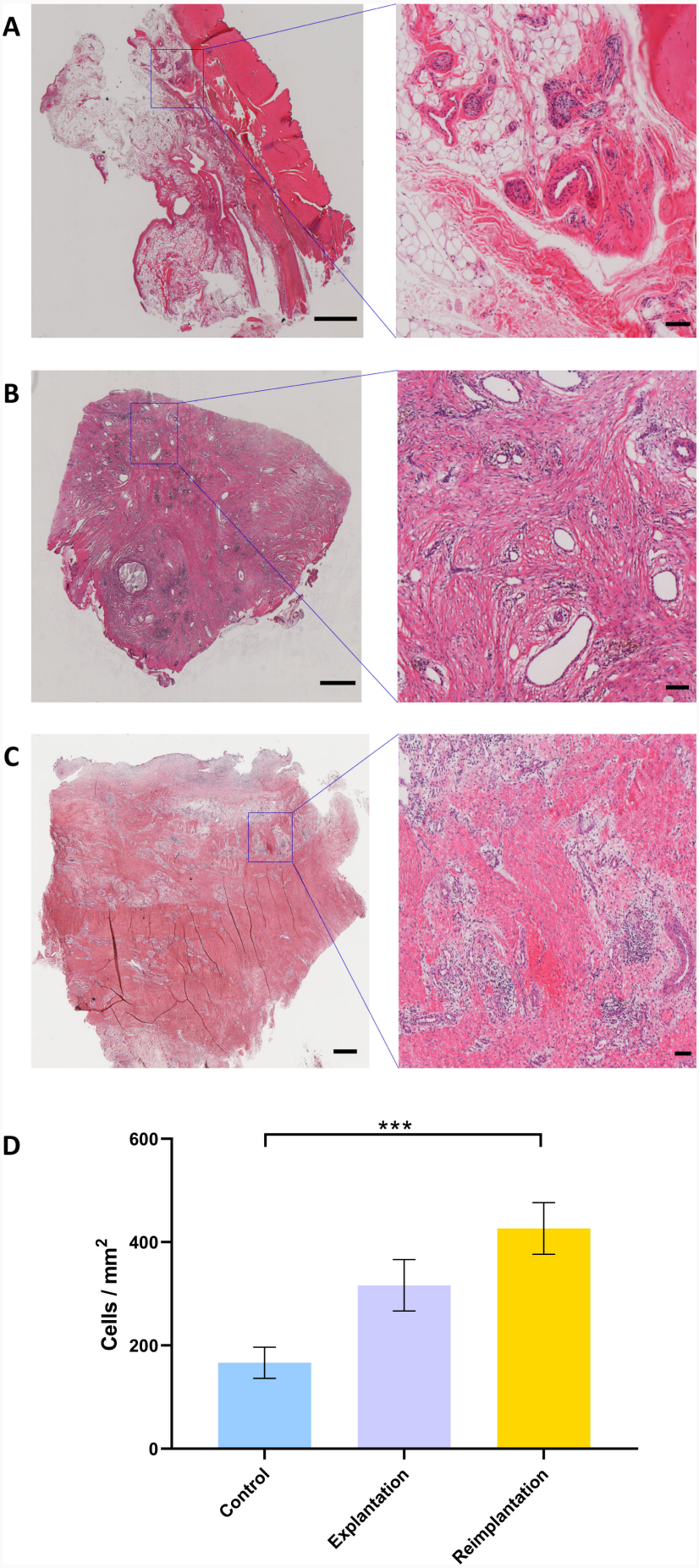

Fig. 1

Increased cellularity in periprosthetic joint infection (PJI). Representative haematoxylin and eosin (H&E) staining of knee capsule tissue from a) control, b) explantation, and c) reimplantation groups. Scale bar represents 1,000 µm for full field, 100 µm for insets. d) Cell count (cells per mm^2). Data are expressed as mean (standard error of the mean). ***$p < 0.001$, Kruskal-Wallis test.

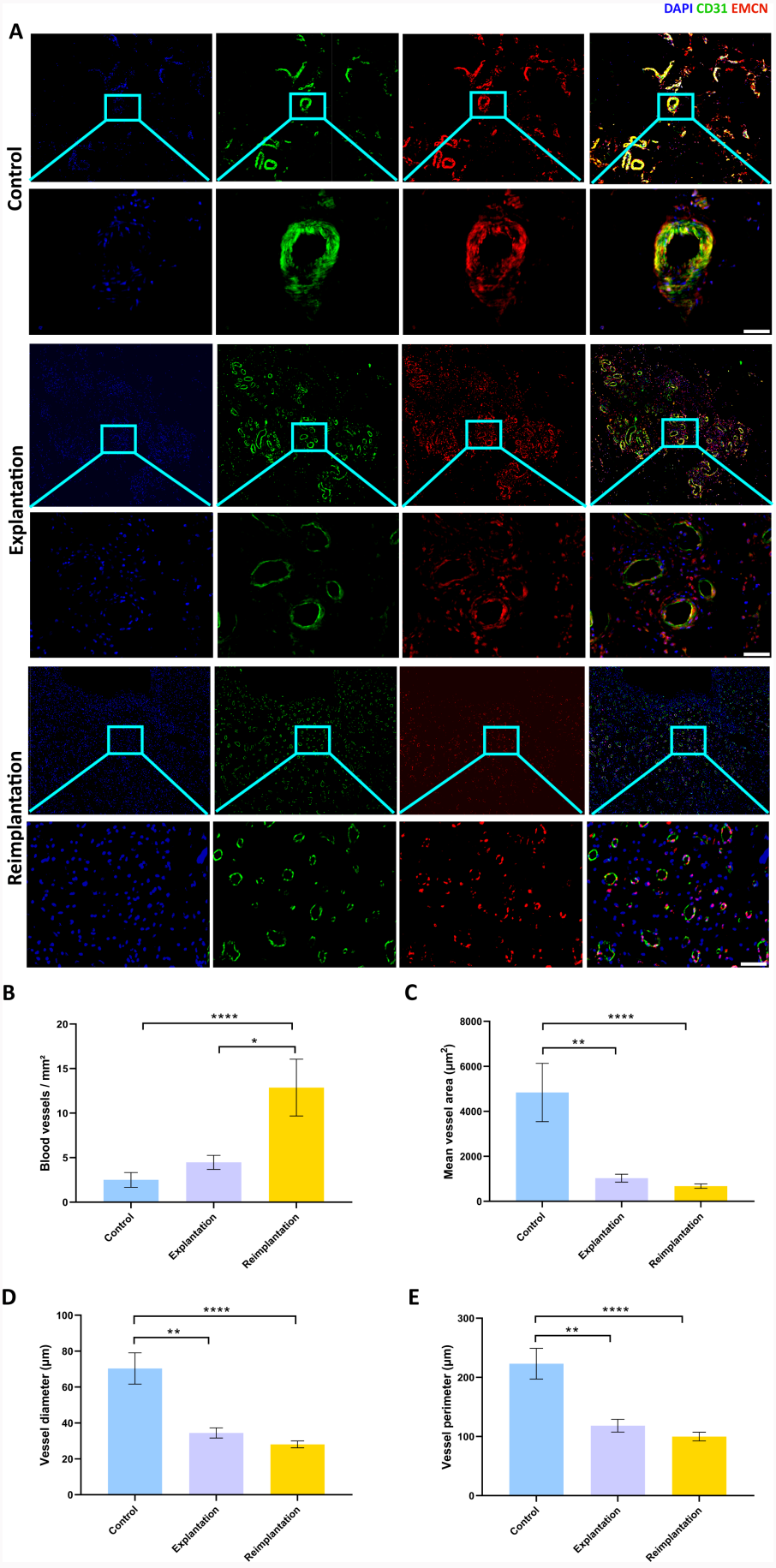

Fig. 2

Vessel number and morphology in periprosthetic joint infection. a) Representative images showing the occurrence and distribution of CD31 and endomucin-stained endothelial cells. Scale bar represents 500 µm for full field, 50 µm for insets. b) Quantification of the number of blood vessels (vessels per mm^2). Quantification of the c) mean vessel area, d) vessel diameter, and e) vessel perimeter. Data are expressed as mean (standard error of the mean). *p < 0.05, **p < 0.01, ****p < 0.0001, Kruskal-Wallis test. DAPI, 4′,6-diamidino-2-phenylindole; EMCN, endomucin.

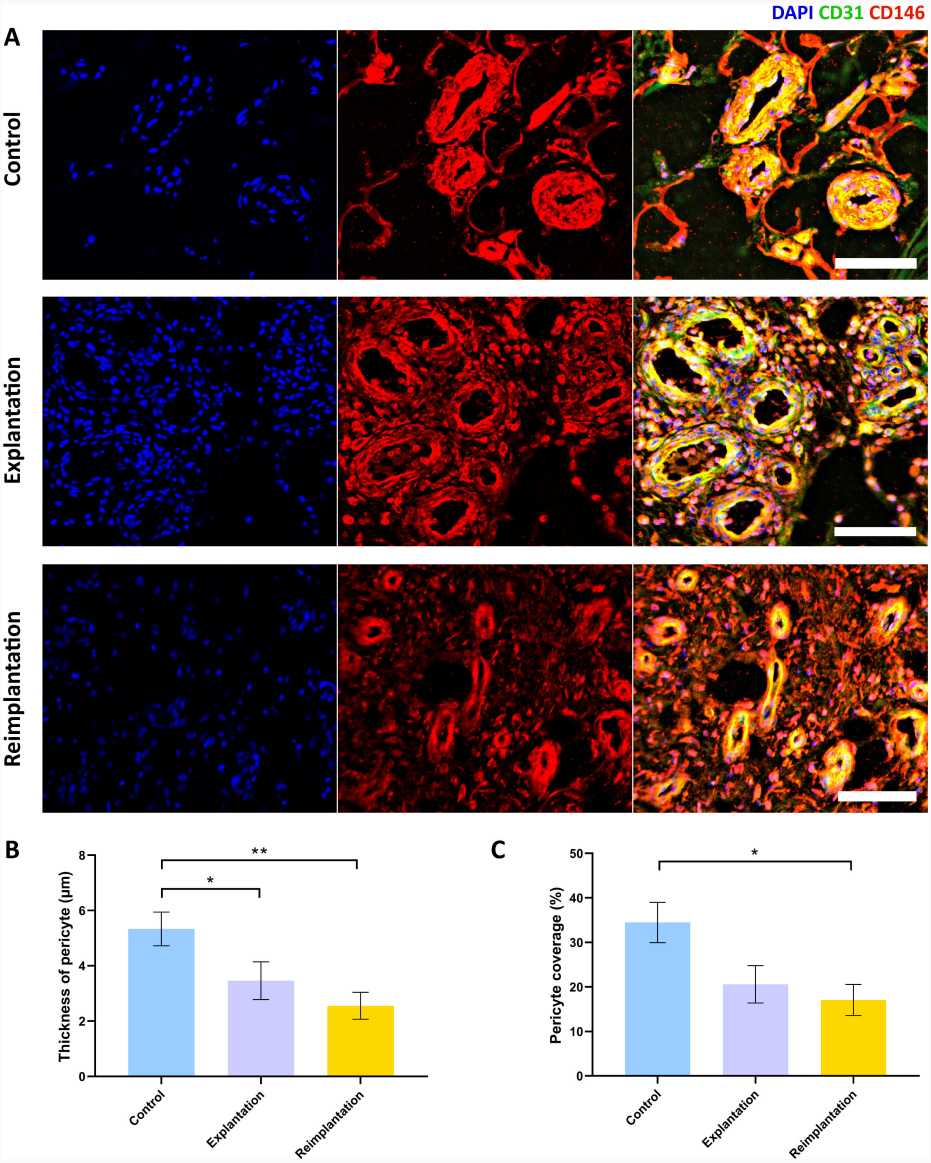

Fig. 3
Pericyte morphology in periprosthetic joint infection. a) Representative images of CD31 and CD146 double stained pericytes. Scale bar 100 µm. Quantification of b) pericyte thickness and c) the area proportion of pericyte in the vessel walls. Data are expressed as mean (standard error of the mean). *p < 0.05, **p < 0.01, Kruskal-Wallis test. DAPI, 4′,6-diamidino-2-phenylindole.

removal and reimplantation. Pericyte thickness was significantly reduced to 3.46 µm (SEM 0.68 (95% CI 2.04 to 4.89); p = 0.029) during prosthesis removal and further decreased to 2.55 µm (SEM 0.49 (95% CI 1.54 to 3.56); p = 0.003) at reimplantation, compared to the control group at 5.33 µm (SEM 0.61 (95% CI 4.07 to 6.60)). However, the proportion of the vessel wall area occupied by pericytes did not show a significant difference during prosthesis removal (20.58% (SEM 4.20 (95% CI 11.84 to 29.31); p = 0.073)), although it was reduced at the time of reimplantation (17.04% (SEM 3.50 (95% CI 9.77 to 24.31); p = 0.017, Kruskal-Wallis test)) compared to the control group (34.47% (SEM 4.52 (95% CI 25.04 to 43.90))).

Smooth muscle cell thickness assessed via alpha-smooth muscle actin (α-SMA) and (endomucin) EMCN co-staining showed a pronounced decrease in PJI (Figure 4): a reduction was observed at both prosthesis explantation and reimplantation, with values of 1.60 µm (SEM 0.33 (95% CI 0.92 to 2.28); p = 0.007) and 1.22 µm (SEM 0.23 (95% CI 0.74 to 1.70); p < 0.001, Kruskal-Wallis test), respectively, compared to the control group at 3.56 µm (SEM 0.56 (95% CI 2.39 to 4.74)). Additionally, the ratio of α-SMA-positive areas within the vessel wall was significantly lower during prosthesis explantation (6.80% (SEM 1.66 (95% CI 3.35 to 10.25); p = 0.002)) and reimplantation (5.87% (SEM 1.23 (95% CI 3.33 to 8.42); p < 0.001, Kruskal-Wallis test)), compared to the control group (20.47% (SEM 3.48 (95% CI 13.19 to 27.75))).

Enhanced fibrotic remodelling and collagen deposition

Sirius Red and Masson's Trichrome staining demonstrated increased collagen deposition in PJI (Figure 5). Quantitative analysis of Sirius Red staining confirmed significantly higher collagen content at explantation (62.51% increase (SEM 5.70 (95% CI 49.82 to 75.21); p = 0.005)) and reimplantation (64.46 (SEM 3.57 (95% CI 56.81 to 72.11); p = 0.001, one-way

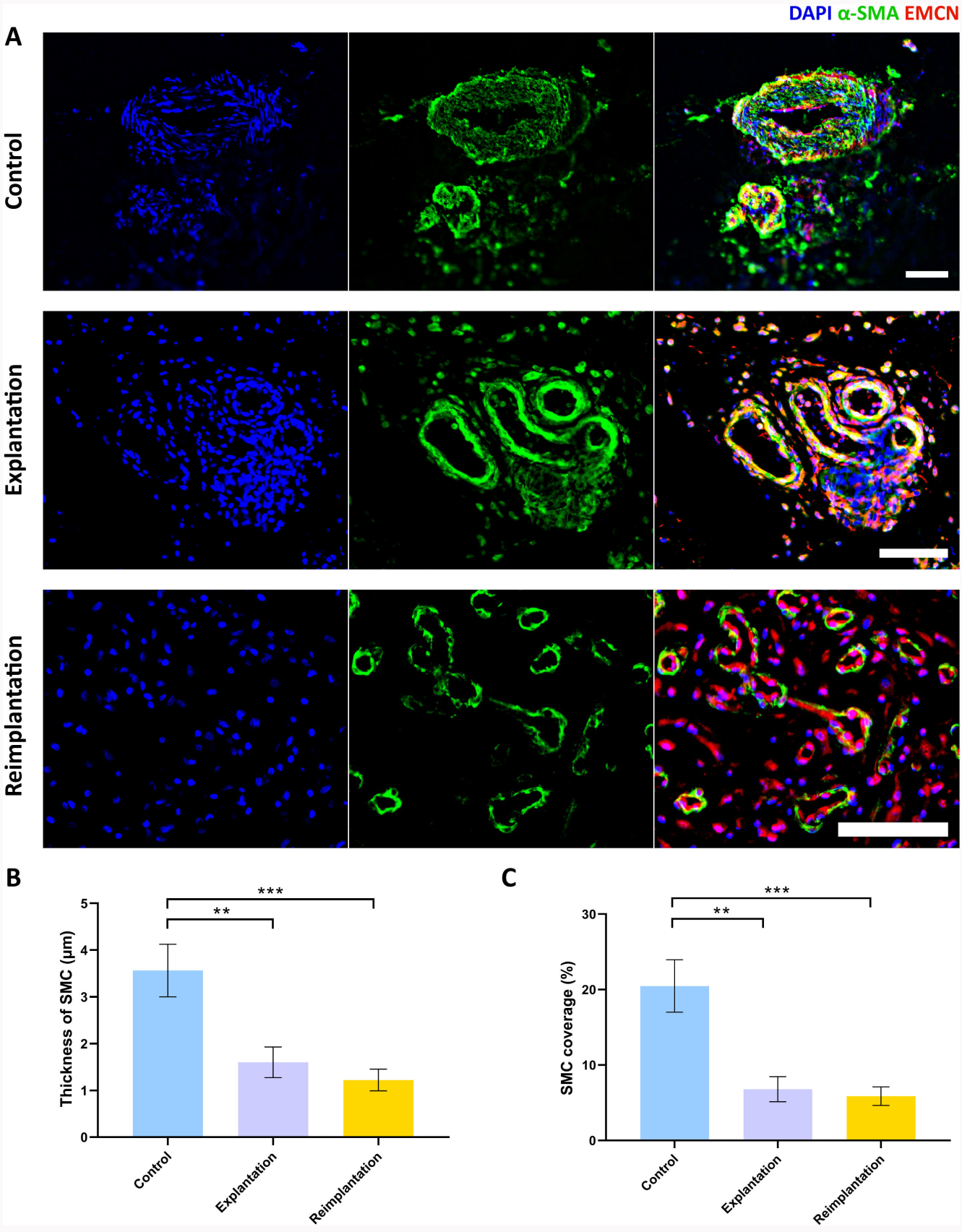

Fig. 4

Vascular remodelling in periprosthetic joint infection. a) Representative images of alpha-smooth muscle actin (α-SMA) and endomucin (EMCN) double-stained joint capsule. Scale bar 100 µm. Quantification of b) smooth muscle cell (SMC) thickness and c) the area proportion of SMC in the vessel walls. Data are expressed as mean (standard error of the mean). **p < 0.01, ***p < 0.001, Kruskal-Wallis test. DAPI, 4′,6-diamidino-2-phenylindole.

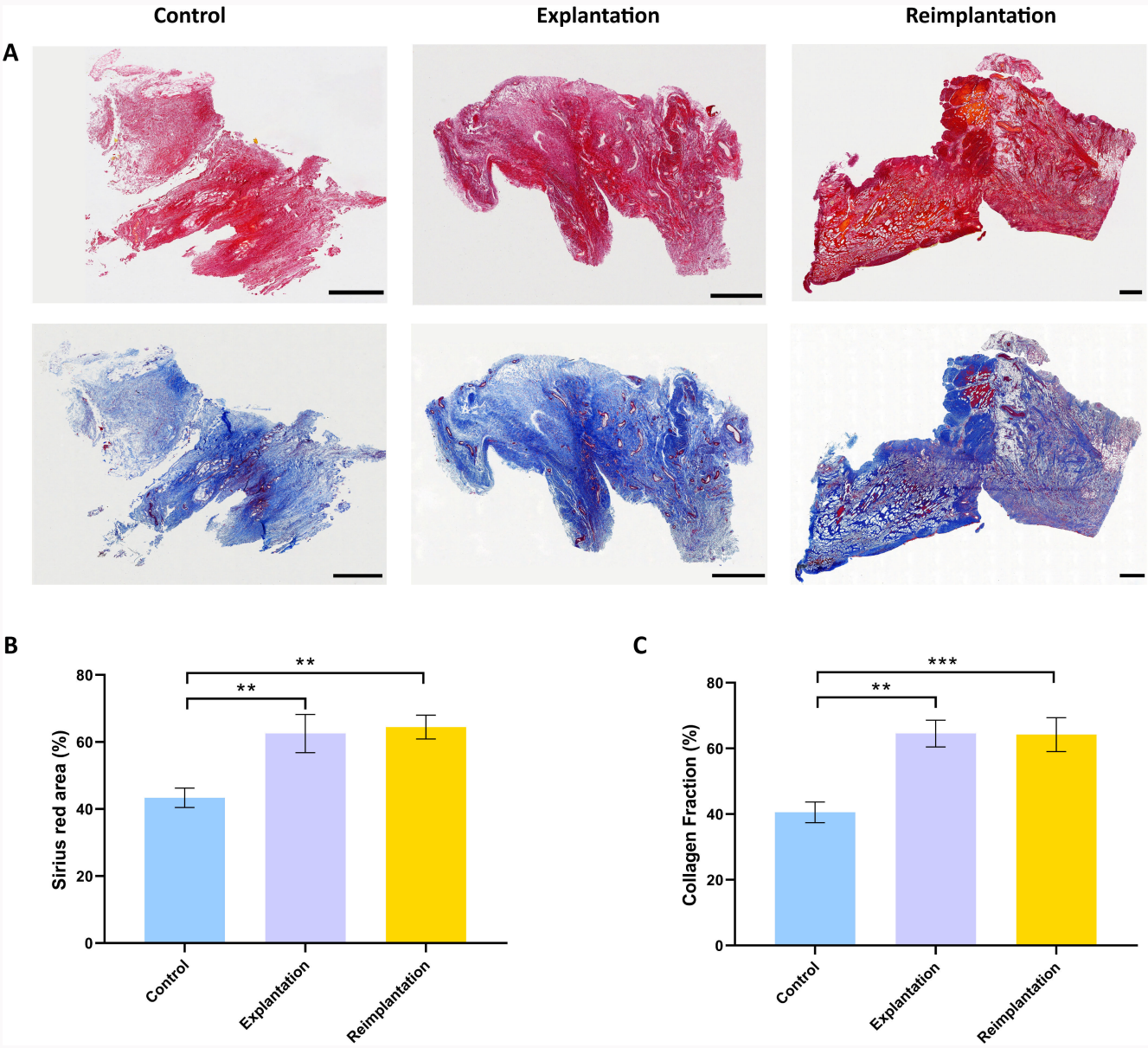

Fig. 5
Histochemical staining for fibrosis analysis. a) Representative pictures of Sirius Red and Masson's trichrome staining showing fibrosis in the control, explantation, and reimplantation groups. Scale bar 1,000 µm. b) Area proportion of Sirius red stained areas. c) Collagen fraction of Masson's trichrome staining. Data are expressed as mean (standard error of the mean). **p < 0.01, ***p < 0.001, one-way analysis of variance.

ANOVA))) compared to the control (43.36 (SEM 2.90 (95% CI 37.03 to 49.69))), with no notable difference between the explantation and reimplantation groups. Similarly, Masson's Trichrome staining showed extensive blue-stained collagen fibres, with quantitative analysis confirming a substantial rise in collagen levels in the explantation (64.55 (SEM 4.06 (95% CI 55.19 to 73.91); p = 0.001)) and reimplantation (64.21 (SEM 5.16 (95% CI 52.86 to 75.57); p < 0.001, one-way ANOVA)) groups compared to the control (40.55 (SEM 3.13 (95% CI 33.67 to 47.43))).

Consistent with these findings, fibronectin expression was significantly elevated in the explantation group (12.37 a.u. (SEM 1.36 (95% CI 9.48 to 15.26))) compared with the control group (6.14 (SEM 1.10 (95% CI 3.59 to 8.68); p = 0.012, one-way ANOVA)), while collagen I levels were markedly increased at both explantation (44.10 (SEM 2.37 (95% CI 39.16 to 49.03); p = 0.002, one-way ANOVA)) and reimplantation (44.97 (SEM 3.57 (95% CI 37.58 to 52.36); p < 0.01)) compared to the control (25.94 (SEM 4.71 (95% CI 16.13 to 35.76)); Figure 6), with all fluorescence images acquired under identical settings to ensure comparability.

Molecular alterations in vascularization, fibrosis, and tissue remodelling

RT-qPCR analysis revealed significant molecular alterations in pathways associated with angiogenesis, extracellular matrix remodelling, and fibrosis (Figure 7). VEGFA expression was significantly reduced at explantation (0.40 (SEM 0.10 (95% CI 0.20 to 0.60); p = 0.002)) and reimplantation (0.54 (SEM 0.11 (95% CI 0.31 to 0.77); p = 0.032, all Kruskal-Wallis test)) compared to the control group (1.00 (SEM 0.17 (95% CI 0.63 to 1.37)); Figure 7a). PDGFA expression was significantly

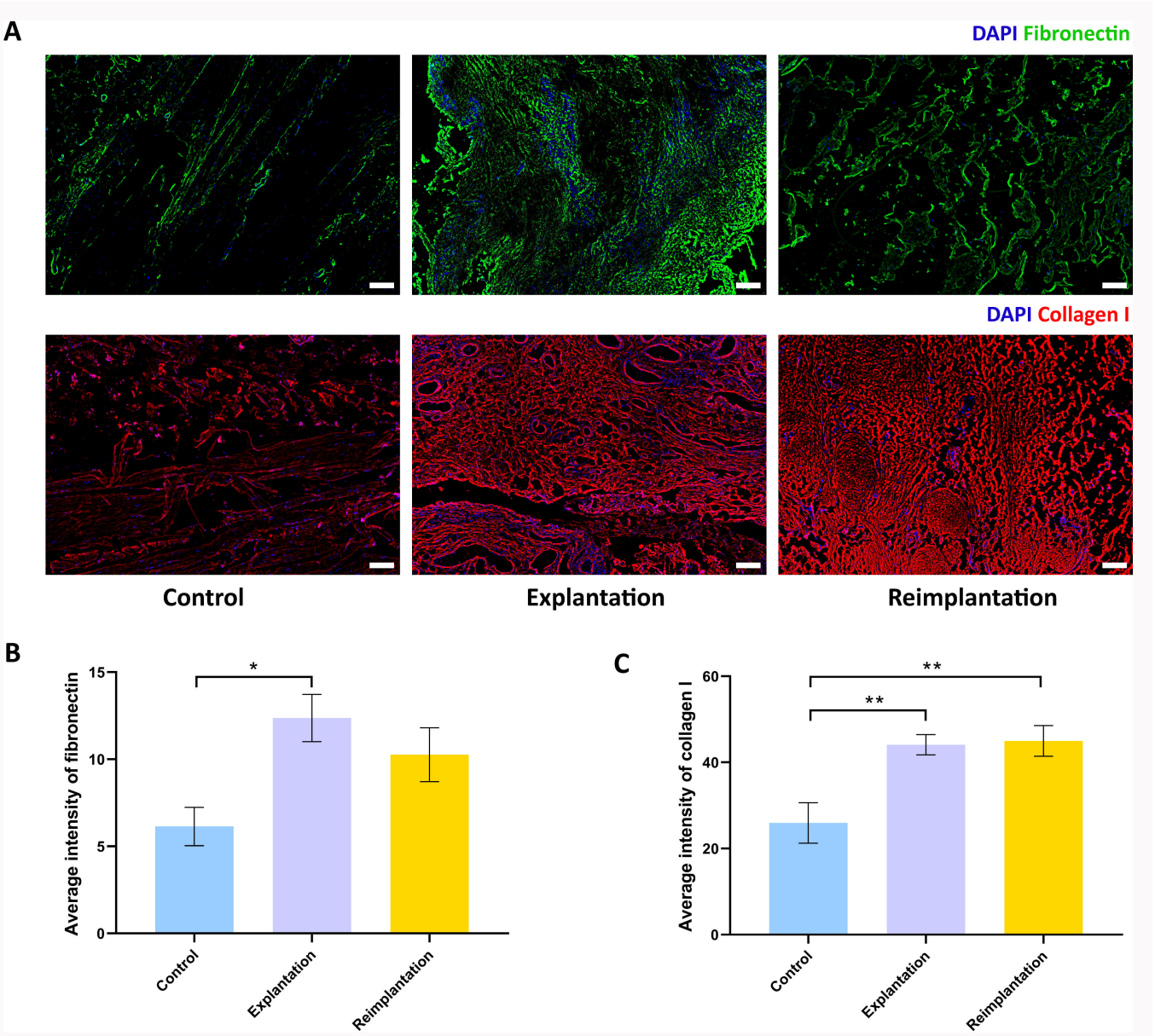

Fig. 6

Immunofluorescence staining of fibronectin and collagen I. a) Representative images of fibronectin (green), collagen I (red), and cell nuclei (blue). Scale bar 200 µm. Quantification of the average intensity of b) fibronectin and c) collagen I. Data are expressed as mean (standard error of the mean). *p < 0.05, **p < 0.01, one-way analysis of variance. DAPI, 4′,6-diamidino-2-phenylindole.

downregulated in the explantation group (0.39 (SEM 0.08 (95% CI 0.22 to 0.55))) compared to the control (1.00 (SEM 0.15 (95% CI 0.68 to 1.32); p = 0.002)). Conversely, there was a marked increase at reimplantation (1.17 (SEM 0.20 (95% CI 0.76 to 1.58); p < 0.001)) compared to the explantation group (Figure 7b). PDGFB was upregulated only at reimplantation versus both control and explantation (p = 0.010 and p = 0.004; Figure 7c). MIG and MMP9 expression levels exhibited a similar pattern: there was no significant difference between the control (MIG: 1.00 (SEM 0.34 (95% CI 0.28 to 1.72)); MMP9: 1.00 (SEM 0.40 (95% CI 0.16 to 1.84))) and explantation (MIG: 1.41 (SEM 0.23 (95% CI 0.91 to 1.91)); MMP9: 1.71 (SEM 0.43 (95% CI 0.80 to 2.63))) groups. In contrast, both genes showed a significant increase in expression at reimplantation (MIG: 2.73 (SEM 0.42 (95% CI 1.86 to 3.60); p < 0.001); MMP9: 6.74 (SEM 1.94 (95% CI 2.75 to 10.73)); p = 0.001) compared to the control (Figures 7d and 7e). COL1A1 expression was significantly elevated in both the explantation group (11.14 (SEM 4.64 (95% CI 1.35 to 20.94); p = 0.035)) and reimplantation group (19.48 (SEM 4.71 (95% CI 9.66 to 29.30); p < 0.001)) compared with the control group (1.00 (SEM 0.27 (95% CI 0.41 to 1.59)); Figure 7f). FN1 expression showed a non-significant reduction in the explantation group (0.39 (SEM 0.09 (95% CI 0.21 to 0.58))) compared to the control group (1.00 (SEM 0.30 (95% CI 0.36 to 1.64); p = 0.737)), but was significantly increased in the reimplantation group (1.30 (SEM 0.25 (95% CI 0.78 to 1.82); p = 0.018); Figure 7g). FGF2 expression was significantly lower in both the explantation group (0.20 (SEM 0.06 (95% CI 0.73 to 1.27); p < 0.001)) and reimplantation group (0.26 (SEM 0.04 (95% CI 0.18 to 0.35); p < 0.001)) compared with the control group (1.00 (SEM 0.13 (95% CI 0.73 to 1.27)); Figure 7h).

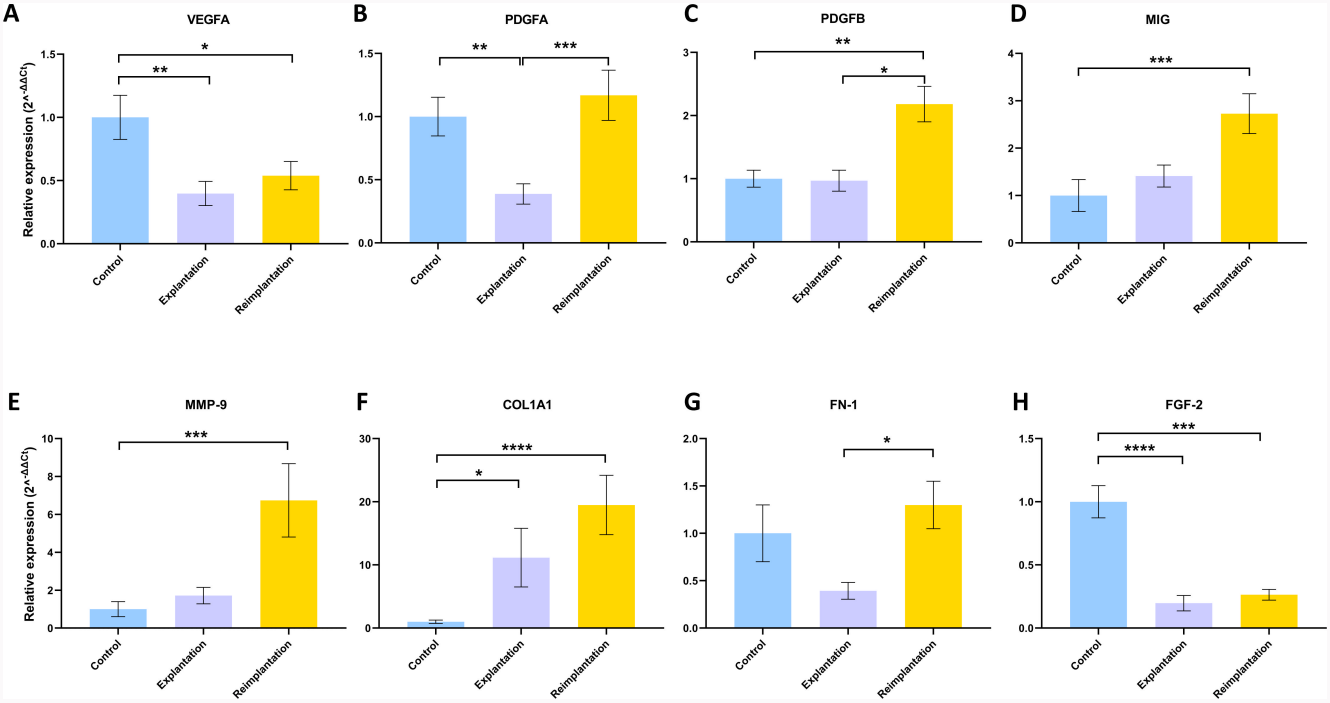

Fig. 7

Molecular alterations associated with vascularization and fibrosis in periprosthetic joint infection. a) Reverse transcription quantitative polymerase chain reaction for vascular endothelial growth factor A (VEGFA), b) platelet-derived growth factor subunit A (PDGFA), c) platelet-derived growh factor subunit B (PDGFB), d) MIG, e) matrix metalloproteinase-9 (MMP-9), f) type I collagen (COL1A1), g) fibronectin 1 (FN-1), and h) fibroblast growth factor 2 (FGF-2). Data are expressed as mean (standard error of the mean). *p < 0.05, **p < 0.01, ***p < 0.001, ****p < 0.0001, Kruskal-Wallis test.

Discussion

In this study, we explored the impact of PJI on vascularization and fibrosis in the joint capsule. Our results indicate that while PJI significantly increased the number of blood vessels, it concurrently led to a reduction in their mean area, diameter, and perimeter during both the prosthetic explantation and reimplantation stages compared to the control group. Additionally, we observed stronger fluorescence signals for fibrosis-associated markers in the explantation and reimplantation groups, consistent with more extensive collagen deposition and suggesting alterations in tissue remodelling. This excessive collagen accumulation may reflect impaired tissue remodelling, which can compromise tissue architecture and immune surveillance, thereby increasing susceptibility to infection as reported in other fibrotic conditions.[14,34,35]

In a previous study, we demonstrated that despite successful treatment of PJI, the risk of prosthesis failure significantly increased, primarily due to recurrent infection or aseptic loosening.[9] Patients with PJI exhibited a sustained and significant increase in proinflammatory markers within the osseous scaffold surrounding their joints.[18] This chronic inflammatory state disrupted normal bone homeostasis, highlighting the potential benefits of targeted interventions to improve long-term clinical outcomes and enhance prosthesis fixation in these patients.[19] However, the effects of this prolonged inflammatory environment on the surrounding soft-tissue structures including the joint capsule remained unknown.

Chronic inflammation and angiogenesis are intricately linked processes. Tissue hypoxia, which commonly occurs in inflamed tissues, is a potent trigger for angiogenesis.[36] The formation of new blood vessels likely serves as a compensatory mechanism, enhancing tissue perfusion and supporting the immune response in the infected area. However, the reduced size and perimeter of individual vessels may indicate irregular patterns of angiogenesis. PJI-associated inflammation adversely affected vascular development and structure, resulting in smaller, less mature neovessels compared to non-infected tissue. Such abnormal vascular structures may hinder efficient immune-cell trafficking and local perfusion, potentially compromising host defense. Similar observations have been reported in other inflammatory and infectious diseases, where altered microvasculature was shown to impair perfusion and immune cell access.[37–39]

Pericyte coverage of vascular sprouts is critical for angiogenesis, as it helps to stabilize and mature the vessel walls, supporting endothelial cell invasion and growth.[40] In the absence of sufficient pericyte or SMC support, newly formed endothelial cell tubes remain unstable and are more susceptible to regression.[41] Our findings revealed a marked difference in the vascular structure in PJI, with a significant reduction in SMC and pericyte thickness, as well as their ratio within blood vessel walls during both prosthetic explantation and reimplantation. Our findings indicate that the immune and inflammatory milieu in PJI is associated with altered vascular components, reflected by reduced angiogenic signalling and structural changes. A loss of smooth muscle cells may reduce vascular tone and elasticity, impairing blood flow, tissue perfusion, and immune surveillance around the prosthesis. Additionally, decreased pericyte coverage may compromise vascular stability and maturation, exacerbating

vascular inflammation and further undermining the integrity of the vascular network.

The ongoing fibrosis observed in both the explantation and reimplantation groups, despite clearing of the infection, suggests a lasting impact of PJI on the joint capsule. Chronic inflammation, driven by both the infection and surgical interventions, likely promotes the excessive accumulation of extracellular matrix (ECM) components, particularly collagen I, which plays a pivotal role in the formation of fibrotic tissue.[42] This altered ECM structure may interfere with the normal repair process and contribute to dysfunction in the affected tissues.[43]

Furthermore, the stiffening of tissues due to excessive collagen buildup can compromise their elasticity, restricting movement and potentially increasing the risk of reinfection or implant failure due to impaired nutrient supply and immunological capacities.[44] A deeper understanding of the underlying mechanisms driving this fibrotic response is essential for developing interventions that target soft-tissue fibrosis in PJI.

The altered expression of angiogenesis-related genes in PJI aligns with the observed structural and functional changes in blood vessels. The significant downregulation of Reduced VEGFA and PDGFA expression following prosthetic explantation suggests impaired angiogenic signalling, which may contribute to reduced vessel area, diameter, and perimeter, consistent with prior findings that PDGF signalling disruption alters pericyte recruitment and vessel morphology.[45,46] The subsequent upregulation of PDGFA and PDGFB at reimplantation indicates an attempt at vascular remodelling; however, the increase in blood vessel numbers without corresponding vessel maturation, as reflected by the decreased SMC and pericyte coverage, suggests an abnormal angiogenic response. The increased expression of MIG and MMP9 at reimplantation suggests an inflammatory and matrix-degrading environment, which may contribute to impaired vascular integrity and excessive tissue remodelling. Elevated COL1A1 expression at explantation and reimplantation, together with increased fibrosis and collagen deposition, indicates persistent ECM remodelling, which may hinder proper tissue regeneration.[47] The reduced expression of FN1 at explantation, followed by an increase at reimplantation, suggests dynamic ECM alterations that could affect cellular adhesion and migration. Notably, the persistent downregulation of FGF2, a key regulator of vascular stabilization and tissue repair, suggests sustained impairment in angiogenesis and regenerative capacity in PJI. This could contribute to delayed tissue healing despite increased vascularization and fibrosis. Overall, these molecular changes indicate a dysregulated balance between angiogenesis, inflammation, and fibrosis, potentially leading to aberrant tissue remodelling in PJI.

This study has several limitations, including a small sample size, patient population heterogeneity, variability in microbial pathogens, an uneven sex distribution between groups, and the use of osteoarthritis controls, which exhibit low-grade inflammation and vascular remodelling that may bias PJI effects toward conservative estimates. Moreover, whether vascular alterations arise as a cause or consequence of PJI cannot be fully determined. Additionally, outcomes such as tissue perfusion, immune cell trafficking, and antibiotic delivery, which may be influenced by vascular remodelling and fibrosis, were not directly assessed, and the potential link to reinfection risk requires further investigation.

Our research highlights significant vascular and fibrotic changes during prosthesis explantation and reimplantation phases. These changes include increased expression of angiogenic markers, ongoing vascular remodelling, and increased fibrotic changes which compromise the structural integrity and function of blood vessels. Such vascular instability and enhanced collagen deposition may weaken immune responses and delay recovery, while potentially hindering effective drug delivery. A deeper understanding of the vascularization and fibrosis associated with PJI is crucial to enhancing therapeutic efficacy, improving antibiotic absorption, and ultimately achieving better clinical outcomes for patients.

Supplementary material

Table detailing the pathogens of patients with periprosthetic joint infection.

References

1. **Kapadia BH**, **Berg RA**, **Daley JA**, **Fritz J**, **Bhave A**, **Mont MA**. Periprosthetic joint infection. *Lancet*. 2016;387(10016):386–394.
2. **Tande AJ**, **Patel R**. Prosthetic joint infection. *Clin Microbiol Rev*. 2014;27(2):302–345.
3. **Grimberg A**, **Kirschner S**, **Lützner J**, **Melsheimer O**, **Morlock M**, **Steinbrück A**. Annual Report 2024, The German Arthroplasty Registry (EPRD). 2024. https://www.eprd.de/fileadmin/user_upload/Dateien/Publikationen/Berichte/AnnualReport2024-Web_2025-03-27_F.pdf
4. **Delanois RE**, **Mistry JB**, **Gwam CU**, **Mohamed NS**, **Choksi US**, **Mont MA**. Current epidemiology of revision total knee arthroplasty in the United States. *J Arthroplasty*. 2017;32(9):2663–2668.
5. **Bhandari M**, **Smith J**, **Miller LE**, **Block JE**. Clinical and economic burden of revision knee arthroplasty. *Clin Med Insights Arthritis Musculoskelet Disord*. 2012;5:89–94.
6. **Kurtz SM**, **Ong KL**, **Lau E**, **et al**. International survey of primary and revision total knee replacement. *Int Orthop*. 2011;35(12):1783–1789.
7. **Dale H**, **Hallan G**, **Espehaug B**, **Havelin LI**, **Engesæter LB**. Increasing risk of revision due to deep infection after hip arthroplasty: a study on 97,344 primary total hip replacements in the Norwegian Arthroplasty Register from 1987 to 2007. *Acta Orthop*. 2009;80(6):639–645.
8. **Kurtz SM**, **Ong KL**, **Lau E**, **Bozic KJ**, **Berry D**, **Parvizi J**. Prosthetic joint infection risk after TKA in the medicare population. *Clin Orthop Relat Res*. 2010;468(1):52–56.
9. **Kienzle A**, **Walter S**, **von Roth P**, **Fuchs M**, **Winkler T**, **Müller M**. High rates of aseptic loosening after revision total knee arthroplasty for periprosthetic joint infection. *JB JS Open Access*. 2020;5(3):e20.00026.
10. **Lin Y-C**, **Chen W-C**, **Peng S-H**, **Chang C-H**, **Lee S-H**, **Lin S-H**. Impact of unplanned second debridement, antibiotics and implant retention on long-term outcomes in knee exchange arthroplasty: elevated risk of failure and reinfection. *J Exp Orthop*. 2024;11(3):e12024.
11. **Karczewski D**, **Scholz J**, **Hipfl C**, **Akgün D**, **Gonzalez MR**, **Hardt S**. Gram negative periprosthetic hip infection: nearly 25% same pathogen infection persistence at a mean of 2 years. *Arch Orthop Trauma Surg*. 2024;144(12):5053–5059.
12. **Triantafyllopoulos GK**, **Memtsoudis SG**, **Zhang W**, **Ma Y**, **Sculco TP**, **Poultsides LA**. Periprosthetic infection recurrence after 2-stage exchange arthroplasty: failure or fate? *J Arthroplasty*. 2017;32(2):526–531.
13. **Ralphs JR**, **Benjamin M**. The joint capsule: structure, composition, ageing and disease. *J Anat*. 1994;184(Pt 3):503–509.
14. **Haywood L**, **Walsh DA**. Vasculature of the normal and arthritic synovial joint. *Histol Histopathol*. 2001;16(1):277–284.
15. **Bai L-K**, **Su Y-Z**, **Wang X-X**, **et al**. Synovial macrophages: past life, current situation, and application in inflammatory arthritis. *Front Immunol*. 2022;13:905356.

16. **Sartawi MM**, **Kohlmann JM**, **Abdelsamie KR**, **Rahman H**. Water-tight arthrotomy joint closure of modified intervastus approach in total knee arthroplasty. *J Clin Med*. 2023;12(12):3985.
17. **Huang J**, **Wang J**, **Qin L**, **Zhu B**, **Huang W**, **Hu N**. Combination of synovial fluid IL-4 and polymorphonuclear cell percentage improves the diagnostic accuracy of chronic periprosthetic joint infection. *Front Surg*. 2022;9:843187.
18. **Biedermann L**, **Bandick E**, **Ren Y**, **et al**. Inflammation of bone in patients with periprosthetic joint infections of the knee. *JB JS Open Access*. 2023;8(1):e22.00101.
19. **Bandick E**, **Biedermann L**, **Ren Y**, **et al**. Periprosthetic joint infections of the knee lastingly impact the bone homeostasis. *J Bone Miner Res*. 2023;38(10):1472–1479.
20. **Schmidt-Bleek K**, **Schell H**, **Schulz N**, **et al**. Inflammatory phase of bone healing initiates the regenerative healing cascade. *Cell Tissue Res*. 2012;347(3):567–573.
21. **Lienau J**, **Schmidt-Bleek K**, **Peters A**, **et al**. Differential regulation of blood vessel formation between standard and delayed bone healing. *J Orthop Res*. 2009;27(9):1133–1140.
22. **Ormsby R**, **Zelmer A**, **Yang D**, **et al**. Evidence for osteocyte-mediated bone-matrix degradation associated with periprosthetic joint infection (PJI). *Eur Cell Mater*. 2021;42:264–280.
23. **Lehmann W**, **Edgar CM**, **Wang K**, **et al**. Tumor necrosis factor alpha (TNF-alpha) coordinately regulates the expression of specific matrix metalloproteinases (MMPS) and angiogenic factors during fracture healing. *Bone*. 2005;36(2):300–310.
24. **Karczewski D**, **Schönnagel L**, **Hipfl C**, **Akgün D**, **Hardt S**. Periprosthetic hip infection in octogenarians: a single institution experience of 33 cases. *Bone Joint J*. 2023;105-B(2):135–139.
25. **Walker LC**, **Clement ND**, **Yapp LZ**, **Deehan DJ**. Change in organism between first- and second-stage revision for periprosthetic joint infection of knee arthroplasty independently associated with increased risk of failure. *Bone Jt Open*. 2023;4(9):720–727.
26. **Yang HY**, **Cheon JH**, **Jung DM**, **Seon JK**. Comparison of outcomes between fungal and non-fungal periprosthetic joint infections in total knee arthroplasty. *Bone Joint J*. 2023;105-B(12):1286–1293.
27. **Straub J**, **Staats K**, **Vertesich K**, **Kowalscheck L**, **Windhager R**, **Böhler C**. Two-stage revision for periprosthetic joint infection after hip and knee arthroplasty: the role of reimplantation histology in reinfection rate. *Bone Joint J*. 2024;106-B(4):372–379.
28. **Lodge CJ**, **Adlan A**, **Nandra RS**, **Kaur J**, **Jeys L**, **Stevenson JD**. Staged revision of the infected knee arthroplasty and endoprosthesis: a retrospective analysis of the failure of antibiotic-loaded cement spacers after the first stage. *Bone Joint J*. 2024;106-B(10):1067–1073.
29. **World Medical Association**. World Medical Association Declaration of Helsinki: ethical principles for medical research involving human subjects. *JAMA*. 2013;310(20):2191–2194.
30. **McNally M**, **Sousa R**, **Wouthuyzen-Bakker M**, **et al**. The EBJIS definition of periprosthetic joint infection: a practical guide for clinicians. *Bone Joint J*. 2021;103-B(1):18–25.
31. **Saklad M**. Grading of patients for surgical procedures. *Anesthesiology*. 1941;2(3):281–284.
32. **Krenn V**, **Morawietz L**, **Perino G**, **et al**. Revised histopathological consensus classification of joint implant related pathology. *Pathol Res Pract*. 2014;210(12):779–786.
33. **Bustin SA**, **Benes V**, **Garson JA**, **et al**. The MIQE guidelines: minimum information for publication of quantitative real-time PCR experiments. *Clin Chem*. 2009;55(4):611–622.
34. **de Zawadzki A**, **Leeming DJ**, **Sanyal AJ**, **et al**. Hot and cold fibrosis: the role of serum biomarkers to assess immune mechanisms and ECM-cell interactions in human fibrosis. *J Hepatol*. 2025;83(1):239–257.
35. **Suárez-Álvarez B**, **Liapis H**, **Anders HJ**. Links between coagulation, inflammation, regeneration, and fibrosis in kidney pathology. *Lab Invest*. 2016;96(4):378–390.
36. **Bunn HF**, **Poyton RO**. Oxygen sensing and molecular adaptation to hypoxia. *Physiol Rev*. 1996;76(3):839–885.
37. **Walsh DA**, **Pearson CI**. Angiogenesis in the pathogenesis of inflammatory joint and lung diseases. *Arthritis Res*. 2001;3(3):147–153.
38. **Szekanecz Z**, **Koch AE**. Vascular involvement in rheumatic diseases: "vascular rheumatology". *Arthritis Res Ther*. 2008;10(5):224.
39. **Woudstra L**, **Juffermans LJM**, **van Rossum AC**, **Niessen HWM**, **Krijnen PAJ**. Infectious myocarditis: the role of the cardiac vasculature. *Heart Fail Rev*. 2018;23(4):583–595.
40. **Helfrich I**, **Schadendorf D**. Blood vessel maturation, vascular phenotype and angiogenic potential in malignant melanoma: one step forward for overcoming anti-angiogenic drug resistance? *Mol Oncol*. 2011;5(2):137–149.
41. **Darland DC**, **D'Amore PA**. Blood vessel maturation: vascular development comes of age. *J Clin Invest*. 1999;103(2):157–158.
42. **Sorokin L**. The impact of the extracellular matrix on inflammation. *Nat Rev Immunol*. 2010;10(10):712–723.
43. **Diller RB**, **Tabor AJ**. The role of the extracellular matrix (ECM) in wound healing: a review. *Biomimetics (Basel)*. 2022;7(3):87.
44. **Kirschbaum S**, **Weynandt C**, **Fuchs M**, **Perka C**, **Gwinner C**. Major shortening of the patellar tendon during septic two-stage knee arthroplasty revision using static spacers. *J Arthroplasty*. 2022;37(9):1851–1857.
45. **Abramsson A**, **Lindblom P**, **Betsholtz C**. Endothelial and nonendothelial sources of PDGF-B regulate pericyte recruitment and influence vascular pattern formation in tumors. *J Clin Invest*. 2003;112(8):1142–1151.
46. **Uutela M**, **Wirzenius M**, **Paavonen K**, **et al**. PDGF-D induces macrophage recruitment, increased interstitial pressure, and blood vessel maturation during angiogenesis. *Blood*. 2004;104(10):3198–3204.
47. **Ricard-Blum S**, **Baffet G**, **Théret N**. Molecular and tissue alterations of collagens in fibrosis. *Matrix Biol*. 2018;68–69:122–149.

Author information

R. Qiao, Cand. med., PhD Candidate
E. Sistemich, Cand. nat., PhD Candidate
Center for Musculoskeletal Surgery, Clinic for Orthopedics, Charité–Universitätsmedizin Berlin, Corporate Member of Freie Universität Berlin, Humboldt-Universität zu Berlin, and Berlin Institute of Health, Berlin, Germany; Julius Wolff Institute and Center for Musculoskeletal Surgery, Charité–Universitätsmedizin Berlin, Corporate Member of Freie Universität Berlin, Humboldt-Universität zu Berlin, and Berlin Institute of Health, Berlin, Germany.

J. Mehl, PhD, Scientist
M. Thiele, MTA, Lab Technician
G. Duda, Prof. Dr., Head of Research Department
Julius Wolff Institute and Center for Musculoskeletal Surgery, Charité–Universitätsmedizin Berlin, Corporate Member of Freie Universität Berlin, Humboldt-Universität zu Berlin, and Berlin Institute of Health, Berlin, Germany.

B. Qi, MD, Physician, Institute of Stomatology, Chinese People's Liberation Army No.989 Hospital, Luoyang, China.

W. Fan, Cand. med., PhD Candidate
S. Kirschbaum, Dr. med., Surgeon
S. Donner, Dr. med., Surgeon
C. Gwinner, PD Dr., Surgeon
C. F. Perka, Prof. Dr., Surgeon, Head of Hospital
Center for Musculoskeletal Surgery, Clinic for Orthopedics, Charité–Universitätsmedizin Berlin, Corporate Member of Freie Universität Berlin, Humboldt-Universität zu Berlin, and Berlin Institute of Health, Berlin, Germany.

D. Jahn, Dr. rer. nat., Researcher, Julius Wolff Institute and Center for Musculoskeletal Surgery, Charité–Universitätsmedizin Berlin, Corporate Member of Freie Universität Berlin, Humboldt-Universität zu Berlin, and Berlin Institute of Health, Berlin, Germany; Department of Oral and Maxillofacial Surgery, Charité–Universitätsmedizin Berlin, Corporate Member of Freie Universität Berlin, Humboldt-Universität zu Berlin, and Berlin Institute of Health, Berlin, Germany.

A. Kienzle, Dr. med., Surgeon, Center for Musculoskeletal Surgery, Clinic for Orthopedics, Charité–Universitätsmedizin Berlin, Corporate Member of Freie Universität Berlin, Humboldt-Universität zu Berlin, and Berlin Institute of Health, Berlin, Germany; Julius Wolff Institute and Center for Musculoskeletal Surgery, Charité–Universitätsmedizin Berlin, Corporate Member of Freie Universität Berlin, Humboldt-Universität zu Berlin, and Berlin Institute of Health, Berlin, Germany; Berlin Institute of Health at Charité–Universitätsmedizin Berlin, BIH Biomedical Innovation Academy, Berlin, Germany.

Author contributions

R. Qiao: Formal analysis, Investigation, Methodology, Writing – original draft.
J. Mehl: Investigation, Visualization.
B. Qi: Formal analysis, Visualization.
E. Sistemich: Data curation, Investigation.
W. Fan: Formal analysis, Writing – review & editing.
S. Kirschbaum: Investigation, Resources, Writing – review & editing.
S. Donner: Investigation, Resources, Supervision, Writing – review & editing.
M. Thiele: Data curation, Methodology.
D. Jahn: Resources, Supervision, Writing – review & editing.
C. Gwinner: Resources, Supervision.
G. Duda: Conceptualization, Funding acquisition, Resources, Supervision.
C. F. Perka: Conceptualization, Funding acquisition, Resources, Supervision.
A. Kienzle: Conceptualization, Funding acquisition, Methodology, Project administration, Supervision, Visualization, Writing – original draft.

Funding statement

The author(s) disclose receipt of the following financial or material support for the research, authorship, and/or publication of this article: R. Qiao was funded by scholarships from China Scholarship Council. A. Kienzle is a participant in the BIH-Charité Clinician Scientist Program funded by the Charité — Universitätsmedizin Berlin and the Berlin Institute of Health.

ICMJE COI statement

R. Qiao reports funding by scholarships from the China Scholarship Council, related to this study. A. Kienzle reports participation in the BIH Charité Clinician Scientist Program funded by the Charité — Universitätsmedizin Berlin and the Berlin Institute of Health, related to this study. The authors declare that the research was conducted in the absence of any commercial or financial relationships that could be construed as a potential conflict of interest.

Data sharing

The data that support the findings for this study are available to other researchers from the corresponding author upon reasonable request.

Open access funding

The open access fee for this article was funded by the Charité Open Access Fund.